

HOx radical regeneration in the oxidation of isoprene

- Supporting Information -

J. Peeters,^{*} T.L. Nguyen, L. Vereecken

Department of Chemistry, K.U.Leuven, Celestijnenlaan 200F, B-3000 Leuven, Belgium

Table of contents

- p. 2: References to quantum chemical and theoretical kinetic methodologies
- p. 3: Addition of OH on isoprene, and isomerisation of chemically activated OH-adducts
- p. 4: O₂ addition on allyl radical CH₂=CH-CH₂•
- p. 5: O₂ addition on hydroxy-isoprene adducts, and redissociation
- p. 7: H-shift reactions in β-OH-ethylperoxy HOCH₂-CH₂-OO•
- p. 8: The 1,5-H-shift reactions 1-OH-2-OO•-isoprene → OH + CH₂O + MVK and 4-OH-3-OO•-isoprene → CH₂O + OH + MACR
- p. 10: Energy trends for the barrier height for 1,5-H-migration in β-OH-peroxy radicals
- p. 12: The 1,6-H-shift reactions in Z-1-OH-4-OO•-isoprene and Z-4-OH-1-OO•-isoprene
- p. 14: Fate of the HOC•H-C(CH₃)=CH-CH₂OOH and HOOCH₂-C(CH₃)=CH-C•HOH radicals
- p. 15: Secondary chemistry: unsaturated hydroperoxide-aldehyde compounds
- p. 18: Secondary chemistry: methyl-vinyl-ketone
- p. 19: Secondary chemistry: methacrolein

References to quantum chemical and theoretical kinetic methodologies

- B3LYP: a) A. D. Becke *J. Chem. Phys.*, 1992, **97**, 9173; b) Lee, A.; Yang, W.; Parr, R. G. *Phys. Rev. B*, 1988, **37**, 785.
- BB1K: Y. Zhao, B. J. Lynch, and D. G. Truhlar, *J. Phys. Chem. A*, 2004, **108**, 2715.
- MPWB1K and MPW1B95: Y. Zhao and D. G. Truhlar, *J. Phys. Chem. A*, 2004, **108**, 6908.
- CBS-QB3: J. A. Montgomery, Jr, M. J. Frisch, J. W. Ochterski, G. A. Petersson, *J. Chem. Phys.*, 1999, **110**, 2822.
- CBS-APNO: J. W. Ochterski, G. A. Petersson, J. A. Montgomery, Jr. *J. Chem. Phys.*, 1996, **104**, 2598.
- CBS(VDZ,VTZ,VQZ): D. Feller and D. A. Dixon, *J. Chem. Phys.*, 2001, **115**, 3484.
- RRKM-Master equations: L. Vereecken; G. Huyberechts; J. Peeters, *J. Chem. Phys.*, 1997, **106**, 6564 (and references therein).

Addition of OH on isoprene, and isomerisation of chemically activated OH-adducts

Addition of OH radicals on the 1- or 4-position of isoprene, yields chemically activated hydroxyadducts where the orientation of the $-\text{CH}_2\text{OH}$ terminal group relative to the CH_2 terminal group can change by internal rotation over the central C–C bond. This central bond is a partial double bond involved in the allyl resonance delocalisation of the free radical electron. Hence, this internal rotation has a comparatively high barrier, about 14-15 kcal/mol, as the double bond needs to be localized to the terminal $-\text{CH}_2=\text{CH}_2$ moiety during rotation, losing the allyl resonance stabilization. Internal rotation is rapid for the nascent OH-isoprene adducts carrying an internal energy of 35-40 kcal/mol (see figure S3), but becomes slow for the thermalized adducts after collisional energy loss. The thermal relative yields of the trans- and cis-adducts are then determined by the steady state concentrations over the higher-energy conformers as they are collisionally thermalized. RRKM-Master equation analysis on these systems reveal that, at temperatures around room temperature (298K) and 1 atm. of air, 1-OH-isoprene adducts are formed in about a 1:1 trans:cis product distribution, while 4-OH addition on isoprene yield a 3:7 adduct conformer ratio.

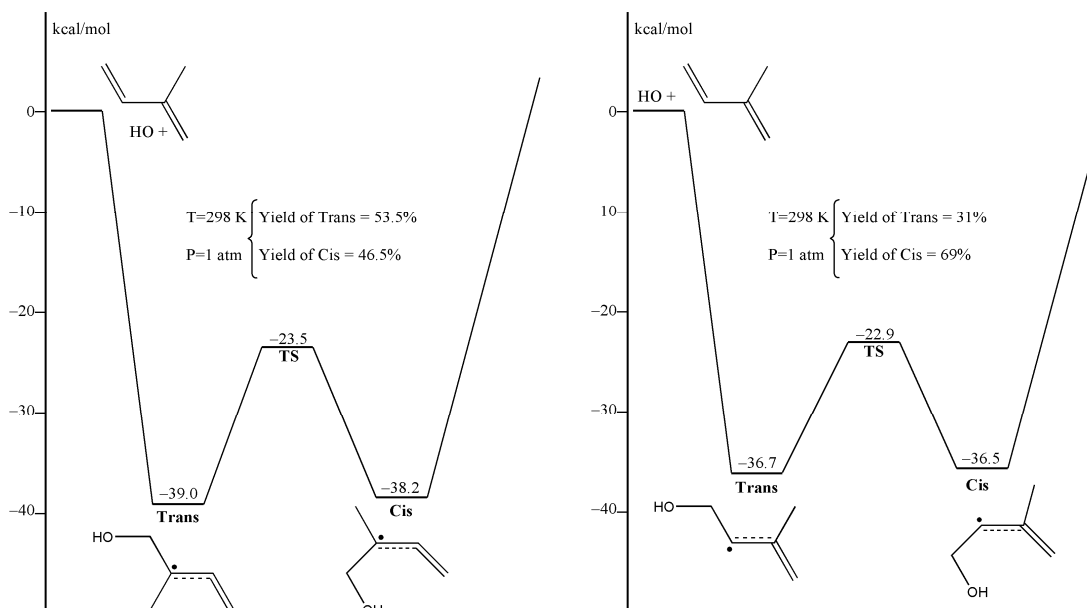


Figure S-3: CBS-APNO energy diagram of the addition of OH on the 1- and 4-position of isoprene, forming cis- and trans conformers of the hydroxy adduct.

O₂ addition on allyl radical CH₂=CH-CH₂[•]

Table S1: Relative energies of the CH₂=CH-CH₂-OO[•] adducts formed after O₂ addition on the allyl radical.

Level of theory	CH ₂ =CH-CH ₂ -OO [•]
MPW1B95	-15.75
CBS-QB3	-18.09 (-19.0 at 298 K)
CBS-QB3 // QCISD/6-311G(d,p)	-18.40
CBS-APNO	-18.37
CC(VDZ,VTZ,VQZ)	-17.73
Exptl. ΔH at 298 K	-18 ± 0.5
Exptl. ΔH converted to 0 K	-17.1 ± 0.5

The well depth of O₂ addition on the allyl radical is determined by the strength of the new bond, and the loss of allyl resonance stabilization of the free radical. DFT-based methodologies have difficulties describing the loss of resonance stabilization, underestimating the experimental data by several kcal/mol. CBS-QB3 and CBS-APNO extrapolation methods, on the other hand, systematically overestimate the well depth compared to the accurately measured experimental reaction enthalpy, where we can convert the 298K enthalpy to a 0K enthalpy with high degree of confidence using the thermal energy contributions derived from the theoretical methodologies. Even the highest-level energy extrapolation we applied, CBS(VDZ,VTZ,VQZ), involving CCSD(T) calculations up to quadruple-zeta basis sets to extrapolate to infinite basis set, still overestimates the addition well depth somewhat compared to the experimental data, but is already in much better agreement.

To be able to reproduce the experimentally measured equilibrium constant for CH₂=CH-[•]CH₂ + O₂ ↔ CH₂=CH-CH₂-OO[•], the CBS-APNO well depth needs to be corrected by 0.9 kcal/mol, while a direct comparison between the CBS-APNO value and the experimentally estimated ΔH(0 K) indicates a 1.25 kcal/mol energy correction on the CBS-APNO addition energy. We propose a weighted average of 1 kcal/mol over these two correction factors for CBS-APNO energies, taking into account that the equilibrium constant measurements are more reliable, and in better agreement over the different determinations. We then systematically correct the CBS-APNO results for O₂ + allyl-type radical addition reactions by 1.0 kcal/mol, as derived here.

O₂ addition on hydroxy-isoprene adducts, and redissociation

The addition of O₂ on allyl radicals was shown earlier to involve a small energy barrier for addition of about 1 kcal/mol. [J. Lee, J.W. Bozzelli, *Proc. Combust. Inst.*, 2005, 30, 1015] For OH-isoprene adducts, the O₂ addition energy profiles show a shallow prereactive complex followed by a broad energy barrier for addition (see Figure S4). For conformers where H-bonding is possible between the O₂ and OH substituents, the barrier remains submerged below the energy level of the separated HO-isoprene + O₂ reactant, while addition of O₂ away from the OH substituent shows a 1 kcal/mol barrier, similar to that found for the allyl radicals. The loss of allyl resonance stabilization results in adduct stabilities comparable to that for allyl+O₂.

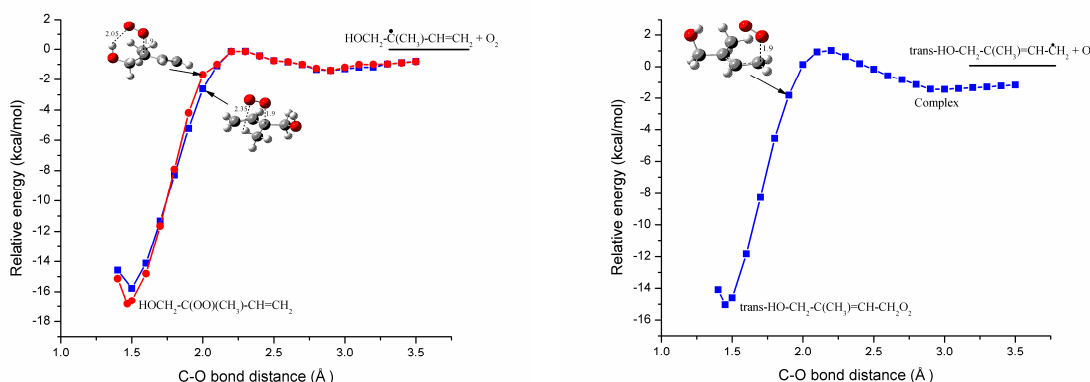


Figure S4: Energy profiles for addition of O₂ on 1-OH-isoprene adducts, calculated at the MPW1B95/6-311++G(3df,3pd) // MPW1B95/6-31+G(d,p) level of theory.

From this, we conclude that formation of E-1-OH-4-OO[•] and E-4-OH-1-OO[•]-isoprene adducts will have a rate constant similar to that for allyl+O₂ per site, i.e. $\sim 0.3 \times 10^{-12}$ cm³ molecule⁻¹ s⁻¹, while the remaining addition channels without an effective barrier, i.e. leading to the Z-isomers or β -OH-O₂ adducts, are significantly faster and make up the bulk of the total measured rate coefficient of 2.3×10^{-12} cm³ molecule⁻¹ s⁻¹ (at 298K) for O₂-addition on HO-isoprene. Furthermore, we propose that the rate coefficient for formation of 1-OH-2-OO[•]-isoprene adducts from either the cis- or trans-OH-isoprene is identical, and likewise for formation of 4-OH-3-OO[•]-isoprene from cis- or trans-4-OH-isoprene. The site-specific rate coefficients for O₂ addition at 303K can then be determined from the total rate coefficient for O₂ addition, and the product distribution measurements under high-NO conditions where the O₂-adducts react immediately with NO to form alkoxy radicals; the yields of methyl-vinyl-ketone, methacrolein, formaldehyde, nitrates, etc. have been measured multiple times.

1-OH-2-O [•] -isoprene (+O ₂) →→ CH ₂ O + HO ₂ + MVK	38%
1-OH-4-O [•] -isoprene (+O ₂) →→ HO ₂ + OCH-C(CH ₃)=CH-CH ₂ OH	22%
4-OH-3-O [•] -isoprene (+O ₂) →→ CH ₂ O + HO ₂ + MACR	20%
4-OH-1-O [•] -isoprene (+O ₂) →→ HO ₂ + HOCH ₂ -C(CH ₃)=CH-CHO	10%
2-OH-1-O [•] -isoprene (+O ₂) →→ CH ₂ O + HO ₂ + MVK	5%
3-OH-4-O [•] -isoprene (+O ₂) →→ CH ₂ O + HO ₂ + MACR	5%

Product	Experimental ^a	Prediction This work
MVK	38 ± 8	40
MACR	25 ± 3	23
CH ₂ O	61 ± 5	63
C ₅ -OH-carbonyl and other carbonyls	30 ± 5	29
Nitrates	8 ± 5	8

^a IUPAC subcommittee for Gas Kinetic Data Evaluation: HO_x + isoprene:
[http://www.iupac-kinetic.ch.cam.ac.uk/datasheets/pdf/HOx_VOC8_HO_CH2C\(CH3\)CHCH2\(isoprene\).pdf](http://www.iupac-kinetic.ch.cam.ac.uk/datasheets/pdf/HOx_VOC8_HO_CH2C(CH3)CHCH2(isoprene).pdf)

The site-specific addition rate coefficients, k_{+O₂}, combined with the theoretically derived equilibrium constants K_{eq}, then leads directly to the rate coefficients for O₂ loss, k_{.O₂}, from the OH-isoprene-O₂ adducts: K_{eq} : k_{+O₂}/k_{.O₂}. Considering the near-absence of an energetic barrier, the rate coefficient for O₂ addition is expected to be only very weakly temperature dependent over a moderate temperature range of 280-320K, such that the T-dependence of the rate coefficients for O₂ loss in OH-isoprene-O₂ adducts is then determined by the T-dependence of the equilibrium constant K_{eq}. The latter can be derived around 298K from Van 't Hoff thermodynamic considerations or from explicit recalculation of partition functions at the temperature considered:

$$\begin{aligned} K_{eq} (\text{cis-1-OH-isoprene} + O_2 \leftrightarrow Z\text{-1-OH-4-OO}^\bullet\text{-isoprene}) &= 1.79 \times 10^{-26} \exp(+8660/T) \text{ cm}^3 \\ K_{eq} (\text{cis-1-OH-isoprene} + O_2 \leftrightarrow 1\text{-OH-2-OO}^\bullet\text{-isoprene}) &= 3.57 \times 10^{-27} \exp(+9970/T) \text{ cm}^3 \\ K_{eq} (\text{trans-1-OH-isoprene} + O_2 \leftrightarrow 1\text{-OH-2-OO}^\bullet\text{-isoprene}) &= 4.00 \times 10^{-27} \exp(+9570/T) \text{ cm}^3 \\ K_{eq} (\text{trans-1-OH-isoprene} + O_2 \leftrightarrow E\text{-1-OH-4-OO}^\bullet\text{-isoprene}) &= 9.80 \times 10^{-26} \exp(+7900/T) \text{ cm}^3 \\ K_{eq} (\text{cis-4-OH-isoprene} + O_2 \leftrightarrow Z\text{-4-OH-1-OO}^\bullet\text{-isoprene}) &= 7.01 \times 10^{-27} \exp(+9110/T) \text{ cm}^3 \\ K_{eq} (\text{cis-4-OH-isoprene} + O_2 \leftrightarrow 4\text{-OH-3-OO}^\bullet\text{-isoprene}) &= 1.82 \times 10^{-27} \exp(+10216/T) \text{ cm}^3 \\ K_{eq} (\text{trans-4-OH-isoprene} + O_2 \leftrightarrow 4\text{-OH-3-OO}^\bullet\text{-isoprene}) &= 3.07 \times 10^{-27} \exp(+10116/T) \text{ cm}^3 \\ K_{eq} (\text{trans-4-OH-isoprene} + O_2 \leftrightarrow Z\text{-4-OH-1-OO}^\bullet\text{-isoprene}) &= 5.38 \times 10^{-26} \exp(+8405/T) \text{ cm}^3 \end{aligned}$$

We thus obtain the following T-dependent redisassociation rate coefficients for the temperature range 280-320 K:

$$\begin{aligned} k_{.O_2} (Z\text{-1-OH-4-OO}^\bullet\text{-isoprene} \rightarrow \text{cis-1-OH-isoprene} + O_2) &= 7.8 \times 10^{13} \exp(-8660/T) \text{ s}^{-1} \\ k_{.O_2} (1\text{-OH-2-OO}^\bullet\text{-isoprene} \rightarrow \text{cis-1-OH-isoprene} + O_2) &= 4.2 \times 10^{14} \exp(-9970/T) \text{ s}^{-1} \\ k_{.O_2} (1\text{-OH-2-OO}^\bullet\text{-isoprene} \rightarrow \text{trans-1-OH-isoprene} + O_2) &= 3.7 \times 10^{14} \exp(-9570/T) \text{ s}^{-1} \\ k_{.O_2} (E\text{-1-OH-4-OO}^\bullet\text{-isoprene} \rightarrow \text{trans-1-OH-isoprene} + O_2) &= 3.1 \times 10^{12} \exp(-7900/T) \text{ s}^{-1} \\ k_{.O_2} (Z\text{-4-OH-1-OO}^\bullet\text{-isoprene} \rightarrow \text{cis-4-OH-isoprene} + O_2) &= 1.4 \times 10^{14} \exp(-9110/T) \text{ s}^{-1} \\ k_{.O_2} (4\text{-OH-3-OO}^\bullet\text{-isoprene} \rightarrow \text{cis-4-OH-isoprene} + O_2) &= 8.25 \times 10^{14} \exp(-10220/T) \text{ s}^{-1} \\ k_{.O_2} (4\text{-OH-3-OO}^\bullet\text{-isoprene} \rightarrow \text{trans-4-OH-isoprene} + O_2) &= 5.0 \times 10^{14} \exp(-10120/T) \text{ s}^{-1} \\ k_{.O_2} (Z\text{-4-OH-1-OO}^\bullet\text{-isoprene} \rightarrow \text{trans-4-OH-isoprene} + O_2) &= 8.65 \times 10^{12} \exp(-8410/T) \text{ s}^{-1} \end{aligned}$$

H-shift reactions in β -OH-ethylperoxy $\text{HOCH}_2\text{--CH}_2\text{--OO}^\bullet$

The migration of the –OH hydrogen to the peroxy radical site has been proposed earlier (K.T. Kuwata, T.S. Dibble, E. Sliz, E.B. Petersen, *J. Phys. Chem. A*, 2007, **111**, 5032.). However, the subsequent dissociation of the alkoxy radical has too high a barrier, 6.8 kcal/mol, to compete effectively at atmospheric temperatures with the reverse reaction, 0.5 kcal/mol. The main fate of the HOO-ethoxy radical is therefore the reverse H-shift to the parent radical.

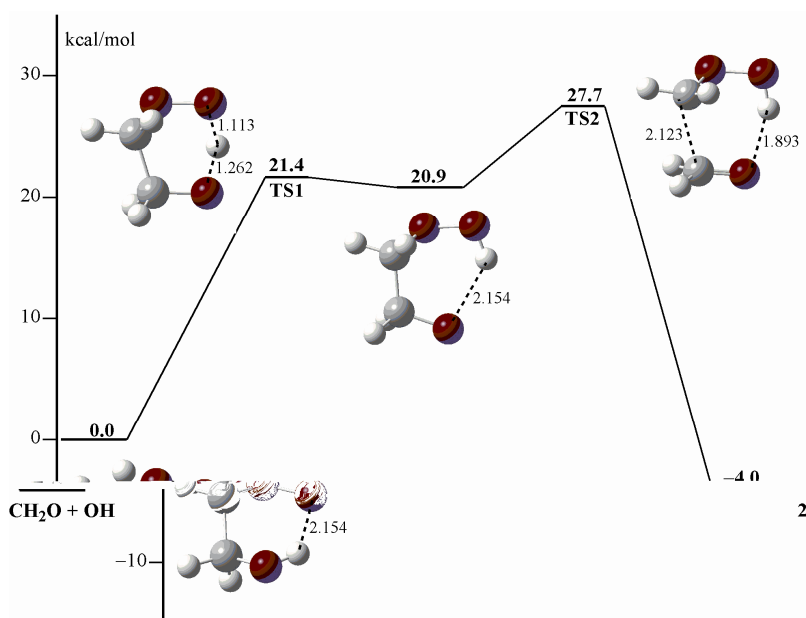
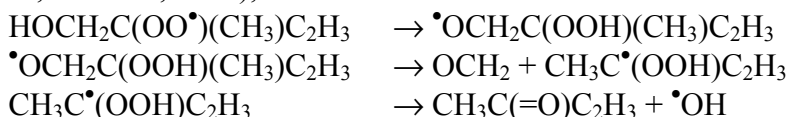


Figure S5: Potential energy surface of the unimolecular reaction of $\text{HOCH}_2\text{CH}_2\text{OO}^\bullet$ calculated at the CBS-APNO level of theory.

The 1,5-H-shift reactions 1-OH-2-OO[•]-isoprene → OH + CH₂O + MVK and 4-OH-3-OO[•]-isoprene → CH₂O + OH + MACR

1-OH-2-OO[•]-isoprene

The migration of the hydroxy-H to the peroxy radical site leads formally to a hydroperoxide-substituted alkoxy radical intermediate, which in turn can eliminate formaldehyde and an α -OOH alkyl radical. These latter radicals have been shown to be thermally unstable (L. Vereecken, T.L. Nguyen, I. Hermans, J. Peeters, Chem. Phys. Lett., 393, 432-436, 2004), and eliminate an OH radical without barrier:



SAR predictions on the alkoxy radical decomposition indicates a barrier of less than 1 kcal/mol for this step, while CBS-QB3 reaction path characterizations show no discernable energy barrier (see figure S8). Hence, once the H-shift transition state energy barrier is cleared, both subsequent reaction steps proceed on a purely repulsive surface without energy barriers, and the overall reaction leads to OH + CH₂O + methylvinylketone directly. The T-dependent rate coefficient for formation of OH+CH₂O+MVK is predicted using multi-conformer transition state theory as $k(T) = 1.52 \times 10^{-11} \exp(-9512/T)$ s⁻¹, including the T-dependent one-dimensional WKB tunneling factor, for the 280 - 320 K range.



Figure S6: QCISD/6-311G(d,p)-optimized geometries of the lowest-lying stationary points for 1,5-H-migration in 1-OH-2-OO[•]-isoprene.

4-OH-3-OO[•]-isoprene

The migration of the hydroxy-H to the peroxy radical site leads formally to a hydroperoxide-substituted alkoxy radical intermediate, which in turn can eliminate formaldehyde and an α -OOH alkyl radical. These latter radicals have been shown to be thermally unstable:



SAR predictions on the alkoxy radical decomposition again indicates a very low barrier of 1.8 kcal/mol or less for this step. Analogous to the reaction above, once the energy barrier for H-shift transition state is cleared, both subsequent reaction steps proceed on a surface without significant energy barriers, and the overall reaction leads to OH + CH₂O + methacrolein directly. The T-dependent rate coefficient for formation of

$\text{OH} + \text{CH}_2\text{O} + \text{methacrolein}$ is predicted using multi-conformer transition state theory as $k(T) = 6.08 \times 10^{-10} \exp(-8893/T) \text{ s}^{-1}$, including the T-dependent one-dimensional WKB tunneling factor, for the 280 - 320 K range.

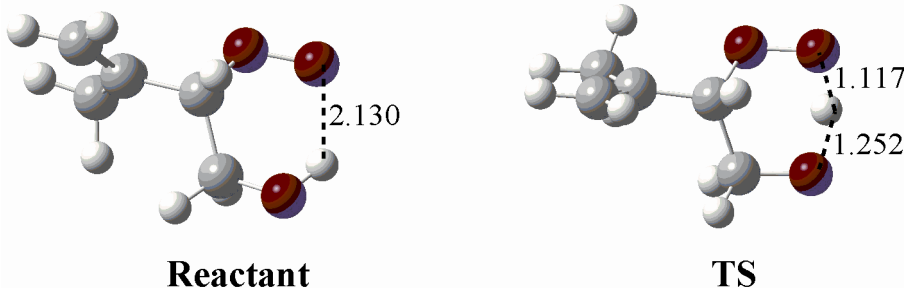


Figure S7: QCISD/6-311G(d,p)-optimized geometries of the lowest-lying stationary points for 1-5-H-migration in 4-OH-3-OO[•]-isoprene

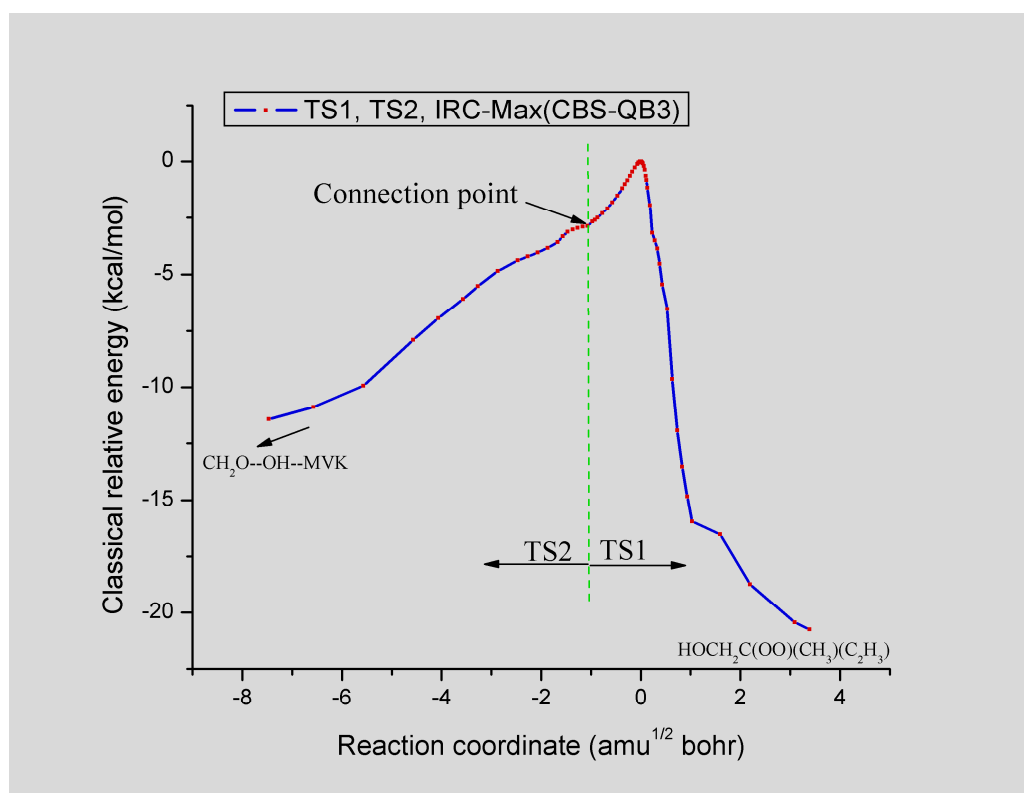
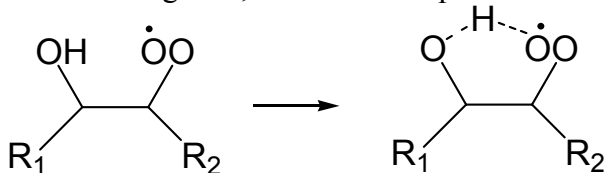


Figure S8: CBS-QB3 characterization of the minimum-energy path of the 1,5-H-shift in 1-OH-2-OO[•]-isoprene (right to left). The figure indicates two transition regimes separated by the dotted vertical line. On the RHS (TS1), the reaction coordinate involves mostly the migration of the hydrogen from the OH to the OO[•] substituents. On the LHS (TS2), the reaction coordinate shifts towards the barrierless decomposition of the hydroxyperoxide-alkoxy radical formally predicted for the reaction sequence. A small shoulder in the otherwise smooth energy profile can be discerned slightly to the left of the dotted line, indicating the position where an alkoxy decomposition TS might be expected.

Energy trends for the barrier height for 1,5-H-migration in β -OH-peroxy radicals

OH-regeneration can occur through a 1,5-H-shift as depicted below:



The third step has been shown to be barrierless for all substitution patterns. Depending on the substituents R_1 and R_2 , the second step can proceed with an additional energy barrier (2-step mechanism), or concerted with the first step without a clearly defined second energy maximum along the reaction coordinate (concerted mechanism). We found that the reaction mechanism becomes concerted when an unsaturated R_2 side group is present (see table S2).

Calculating the energy barrier for this process accurately proved difficult, and prone to systematic errors (see table S2). As expected, the B3LYP barrier height for this H-migration underestimates the predictions of higher level of theories. BB1K, MPW1K and MPWB1K DFT-functionals yield results much closer the higher-level CBS calculations, but seem to overestimate the barrier height somewhat. For the CBS-QB3 calculations, we find a systematic and pronounced trend towards lower energy barriers upon improvement of the geometry, from DFT/MP2 towards QCI-based geometries. Likewise, improving the CBS energy extrapolation step from QB3 to APNO again leads systematically to lower barrier heights for H-migration. This leads us to believe that the barrier heights, even at the costly CBS-APNO level of theory, are not converged with respect to geometry and basis set extrapolation, and represent an upper limit estimate only. Higher-level calculations are in progress to test this hypothesis.

The reason for the sensitivity to the transition state geometry is likely to be related to the bent, non-linear H-migration trajectory, such that uncertainties on the geometry optimization not only shifts the TS along the reaction coordinate; but also tends to shift the estimated TS geometry away from the true minimum energy pathway, leading to higher energy estimates. The bent trajectory for migration also affects tunneling predictions along this trajectory, with one-dimensional estimates such as WKB inherently underestimating the tunneling contribution. A multi-dimensional tunneling correction, such as small-curvature tunneling, is more appropriate. Unfortunately, to be accurate, such SCT calculations would need to be performed on a potential energy surface obtained at very high levels of theory, to obtain the correct reaction path (see above); such calculations are computationally expensive and beyond the scope of the current work.

Table S2: Barrier heights for 1,5-H-migration in a series of substituted hydroxyperoxy radicals, at various levels of theory.

Level of theory	Ethene R ₁ = H R ₂ = H	Propene R ₁ = H R ₂ = CH ₃	butadiene R ₁ = H R ₂ = CH=CH ₂	Isoprene R ₁ = CH ₃ R ₂ = CH=CH ₂	Isoprene R ₁ = H R ₂ = C(CH ₃)=CH ₂
Mechanism	2-step	2-step	concerted	concerted	concerted
B3LYP/6-311++G(3df,3pd)	18.8	17.8	17.1	17.7	16.9
// B3LYP/6-311G(d,p)					
BB1K/6-311++G(3df,3pd)	23.5	22.8	22.2	22.8	21.9
// BB1K/6-31+G(d,p)					
MPWB1K/6-311++G(3df,3pd)	24.0	23.2	22.6	23.2	22.3
// MPWB1K/6-31+G(d,p)					
MPW1K/6-311++G(3df,3pd)	24.2	23.6	23.0	23.7	22.6
// MPW1K/6-311++G(d,p)					
CBS-QB3	23.6	22.1	21.14	21.2	20.6
// B3LYP/6-311G(d,p)					
CBS-QB3	22.6	21.24	21.08	21.8	
// MP2/6-311G(d,p)					
CBS-QB3	21.8	20.9	20.33	20.9	20.0
// QCISD/6-311G(d,p)					
CBS-APNO	21.4	20.54	20.07	20.9	19.74

The 1,6-H-shift reactions in Z-1-OH-4-OO[•]-isoprene and Z-4-OH-1-OO[•]-isoprene

* Z-1-OH-4-OO[•]-isoprene

The temperature-dependent rate coefficient around 298K for the 1,6-H-migration in Z-1-OH-4-OO[•]-isoprene can be derived from multi-conformer transition state theory calculations, using the CBS-APNO barrier height (see table S3), and one-dimensional WKB tunneling corrections: $k(\text{Z-1-OH-4-OO}^{\bullet}\text{-isoprene} \rightarrow \text{HOCH}_2\text{C(CH}_3\text{)=CH-CH}_2\text{OOH}) = 9.82 \times 10^8 \exp(-6303/T) \text{ s}^{-1}$, for the 280 - 320 K range.

Table S3: Barrier heights for 1,6-H-migration in Z-1-OH-4-OO[•]-isoprene \rightarrow HOCH[•]C(CH₃)=CH-CH₂OOH at various levels of theory

Level of theory	Barrier height (kcal/mol)
B3LYP/6-31+G(d,p)	16.32
CBS-QB3	17.10
CBS-QB3 // QCISD/6-311G(d,p)	17.42
CBS-APNO	17.95

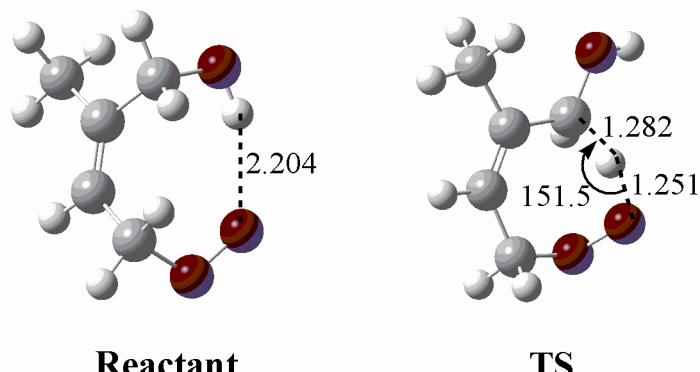


Figure S9: QCISD/6-311G(d,p)-optimized geometries of the lowest-lying conformers of the reactant Z-1-OH-4-OO[•]-isoprene and the 1,6-H shift transition state.

* Z-4-OH-1-OO[•]-isoprene

The temperature-dependent rate coefficient around 298K for the 1,6-H-migration in Z-4-OH-1-OO[•]-isoprene can be derived from multi-conformer transition state theory calculations, using the CBS-APNO barrier height (see table S4), and one-dimensional WKB tunneling corrections: $k(\text{Z-4-OH-1-OO}^{\bullet}\text{-isoprene} \rightarrow \text{HOOCH}_2\text{-C(CH}_3\text{)=CH-C}^{\bullet}\text{HOH}) = 7.32 \times 10^8 \exp(-5556/T) \text{ s}^{-1}$, for the 280 - 320 K range.

Table S4: Barrier heights for 1,6-H-migration in Z-4-OH-1-OO[•]-isoprene → HOOCH₂-C(CH₃)=CH-C[•]HOH at various levels of theory

Level of theory	Barrier height (kcal/mol)
B3LYP/6-31+G(d,p)	14.30
CBS-QB3	15.91
CBS-QB3 // QCISD/6-311G(d,p)	16.03
CBS-APNO	16.26

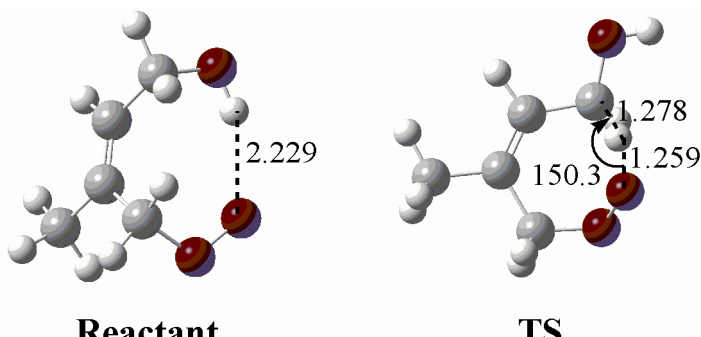


Figure S10: QCISD/6-311G(d,p)-optimized geometries of the lowest-lying conformers of the reactant Z-4-OH-1-OO[•]-isoprene and the 1,6-H shift transition state.

Fate of the HOC[•]H-C(CH₃)=CH-CH₂OOH and HOOCH₂-C(CH₃)=CH-C[•]HOH radicals

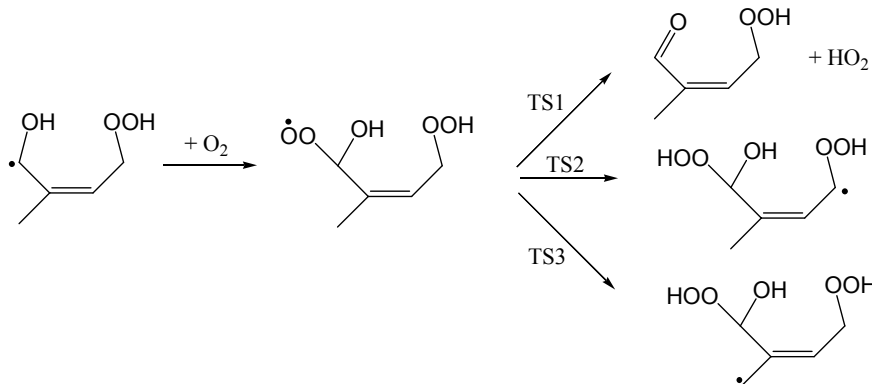


Figure S11: Reaction of an α -OH alkyl radical with O_2 : possible reaction routes

The α -OH alkyl radicals formed after 1,6-H-migration in Z-1-OH-4-OO[•]-isoprene and Z-4-OH-1-OO[•]-isoprene will react with O_2 , forming an α -OH peroxy radical. As is typical for this type of radicals, the dominant reaction is elimination of an HO_2 radical, forming a carbonyl compound (TS1). Alternative reactions, such as a 1,6-H-shift (TS2) and a 1,5-H-shift (TS3), are not competitive, with high energetic barriers (see table S5).

Table S5: barrier heights (kcal/mol) for reactions of the α -OH peroxy radicals formed in the OH-initiated oxidation of isoprene in pristine forest conditions.

TS	B3LYP	CBS-QB3
TS1 - HO_2 elimination	4.5	9.9
TS2 - 1,6-H-shift	16.3	17.7
TS3 - 1,5-H-shift	22.9	23.2

Secondary chemistry: unsaturated hydroperoxide-aldehyde compounds

The unsaturated hydroperoxide-aldehyde compounds formed from Z-1-OH-4-OO[•]-isoprene and Z-4-OH-1-OO[•]-isoprene react mostly either by reaction with OH radicals, i.e. abstraction of the aldehydic or an α -OOH hydrogen, or by photodissociation. Of these, photodissociation is expected to be the dominant fate, owing to the α,β -unsaturated aldehyde moiety, HC(O)-C(CH₃)=CH- or HC(O)-CH=C(CH₃)-, known to have a large photon absorption cross section with a maximum (of about 7×10^{-20} cm²) around 330 nm, and still very large up to 360 nm, as well-documented for the α,β -unsaturated aldehydes metacrolein and methylvinylketone (see IUPAC database [http://www.iupac-kinetic.ch.cam.ac.uk/show_datasheets.php?category=Organic+photolysis]).

The general mechanism of photodissociation of aldehydes was discussed by Moore and Weisshaar [C. B. Moore and J. C. Weisshaar, *Annu. Rev. Phys. Chem.*, 1983, **34**, 525] for H₂CO, and by Leu et al. [G.H. Leu et al., *J. Chem. Phys.*, 1998, **109**, 9340] among others for CH₃CHO. It involves the excitation of the singlet ground state to an excited singlet state upon photon absorption, S₀ + h ν → S₁, followed by fast internal conversion (IC) of the excited S₁ state to the vibrationally highly excited S₀^{*} ground state: S₁ → S₀^{*}, or by reversible intersystem crossing (ISC) to the vibrationally excited triplet state: S₁ ↔ T₁^{*}. Then, as in chemical activation, the internal energy is randomized over all modes within $\sim 10^{-12}$ s, whereupon subsequent unimolecular chemistry of S₀^{*} or T₁^{*} can proceed in competition with collisional thermalization (pressure-quenching); such activated process are commonly and successfully modeled in RRKM-Master Equation theoretical-kinetic analyses. This competition between unimolecular reactions versus quenching is in agreement with the known pressure-dependent photo-dissociation quantum yields of carbonyls.

The S₁ → S₀^{*} IC step is known to be the most important S₁ depopulation process at low S₁ energies, i.e. for S₁ vibration levels lying below or not too far above the dissociation limits of the S₀ state; this should be the case for the conjugated, unsaturated aldehydes of interest here with their markedly smaller S₁ - S₀ gap of only ≈ 70 kcal/mol, upon absorbing photons in the 320 - 370 nm range where the absorption cross section is still close to its maximum (around 335 nm) and where the BL photon flux becomes larger.

For absorption of a 330 nm photon, the internal energy prior to any collisional quenching is nearly ~ 90 kcal/mol (including a few kcal/mol initial thermal energy), which is barely sufficient to break a regular C-C bond or the aldehydic C-H bond, leading for larger molecules to slow dissociation rates in comparison to collisional energy loss and hence a low photodissociation yield. This is found e.g. for methacrolein with a low effective quantum yield of 0.003 - 0.005 [see S. P. Sander, et al., Chemical Kinetics and Photochemical Data for Use in Atmospheric Studies, Evaluation No. 15, Publication 06-2, Jet Propulsion Laboratory, Pasadena, 2006]. The unsaturated hydroperoxide-aldehyde compounds studied here, however, have a very weak O-O bond in the -OOH moiety, only ~ 40 kcal mol⁻¹, and RRKM-type estimates of the dissociation rate coefficients indicate that even for absorption of a low-energy photon of 360 nm, i.e. equivalent to only ~ 83 kcal mol⁻¹ internal energy, the O-O bond will readily break, at rates exceeding or at least very competitive with collisional quenching.

Hence, photodissociation rates for the unsaturated hydroperoxide-aldehyde compounds of interest are expected to be very high, around $J = 3 \times 10^{-4} \text{ s}^{-1}$, and to lead to ~100% generation of an $\cdot\text{OH}$ radical (see figure S12).

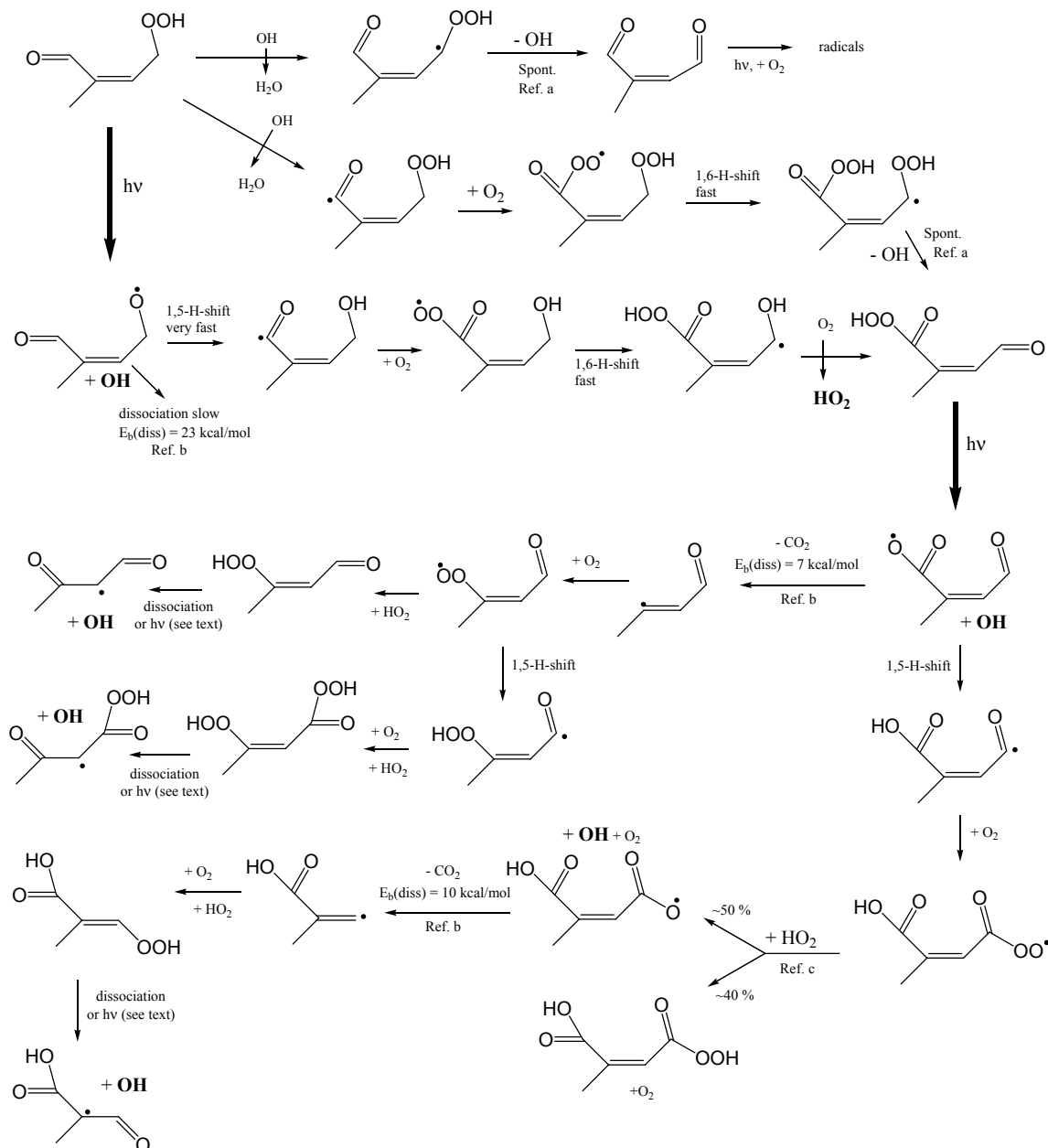


Figure S12: Subsequent chemistry of the hydroperoxy-aldehyde compound formed in a 1,6-H-shift reaction from Z-1-OH-4-OO[•]-isoprene.

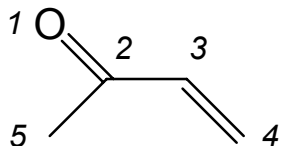
It may be noted that O–OH dissociation can also occur from the T_1^* state, $\bullet\text{O}-\text{C}_a\text{H}=\text{CR}-\text{C}\bullet\text{H}-\text{C}_a\text{H}_2-\text{OOH}$, via a Norrish type II mechanism, in which the $\bullet\text{O}-\text{C}$ radical site abstracts one of the α' -hydroperoxide H-atoms, resulting here in an unstable triplet α -hydroxy- α' -hydroperoxy (bi)radical, $\text{HO}-\text{C}_a\bullet-\text{C}=\text{C}-\text{C}_{a'}\bullet-\text{OOH}$, that spontaneously decomposes [ref d] by expelling the OH (on the right) to form a first aldehyde functionality, followed by O_2 attack on the α -hydroxy-site to form a second aldehyde function plus an HO_2 radical.

Returning to the more probable O–OH homolysis on the S₀* surface, discussed higher, the subsequent chemistry of the unsaturated alkoxy radical formed is shown in figure S12, and involves several easy isomerisation steps involving the weakly bonded aldehydic-H or α -OH hydrogen. The first closed shell molecule formed is an unsaturated peroxyacid-aldehyde that, similar to above, is again expected to have a high photon absorption cross section owing to the O=C–C=C chromophore, and a very high dissociation quantum yield due to the weak O–O bond of ~40 kcal mol⁻¹. This will lead to additional •OH radical formation in its photochemistry (see figure S12, minor reactions of this compound with OH radicals not shown). The subsequent degradation chemistry depends on the competition between CO₂ elimination versus 1,5-H-shift in the unsaturated acyloxy radical O=C(O[•])-C(CH₃)=CHCHO, and high-level quantum chemical calculations are needed to quantify this competition. In any case, the intermediates formed are low-volatility α,β -unsaturated carbonyl compounds with a hydroperoxide or peracid functionality, likely to again be susceptible to OH-generating photodissociation as detailed above. Alternatively, or in the case without the unsaturated aldehyde O=C–C=C chromophore, the thermal decomposition of α,β -unsaturated hydroperoxides can release an •OH radical; the barrier for the unimolecular O–O bond scission has been calculated to be less than ~17 kcal mol⁻¹, owing to the exothermic formation of a delocalized 2-oxo-alkyl radical with vinoxy-resonance stabilization [see e.g. T.L. Nguyen, J. Peeters, L. Vereecken, *Phys. Chem. Chem. Phys.*, in press (2009) DOI: [10.1039/B822984H](https://doi.org/10.1039/B822984H).] Both of these subsequent chemistries would replenish the radical HO_x pool, generating large amounts of OH radicals, and (more than) compensate for the HO₂ loss earlier in the reaction scheme.

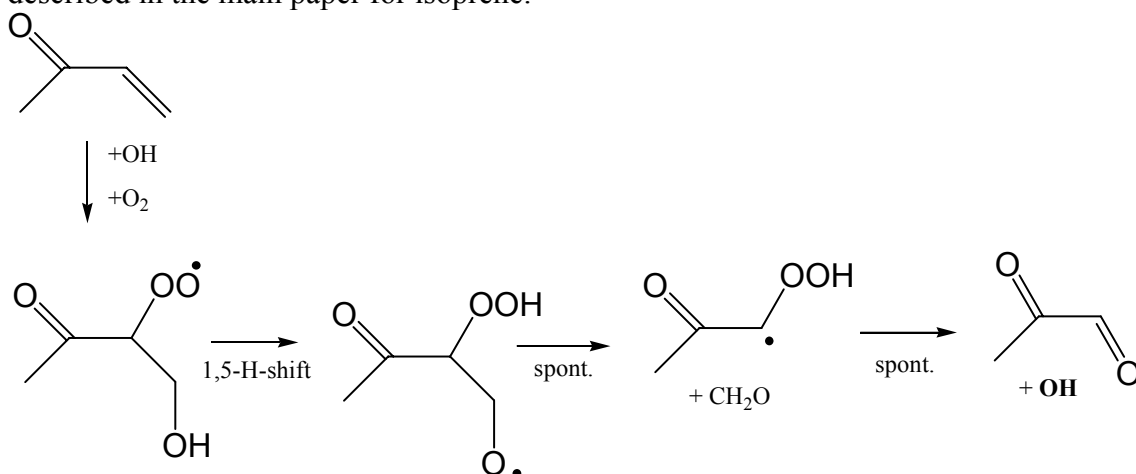
- Ref a: I. Hermans, J. F. Müller, T. L. Nguyen, P. A. Jacobs, and J. Peeters, *J. Phys. Chem. A*, 2005, **109**, 4303.
Ref b: a) J. Peeters, G. Fantechi, and L. Vereecken, *J. Atmos. Chem.*, 2004, **48**, 59-80, 2004; b) L. Vereecken, and J. Peeters, manuscript in preparation.
Ref c: T.J. Dillon, J.N. Crowley, *Atmos. Chem. Phys.*, 2008, **8**, 4877.
Ref d: L. Vereecken, T.L. Nguyen, I. Hermans, J. Peeters, *Chem. Phys. Lett.*, 2004, **393**, 432

Secondary chemistry: Methyl-vinyl-ketone

Labeling of methyl-vinyl-ketone atoms is done here analogous to isoprene in the main paper:



The OH-initiated oxidation of MVK might regenerate OH by an analogous process as described in the main paper for isoprene:



The barrier height for the H-shift is predicted at 20.03 kcal/mol. MC-TST calculations, incorporating WKB tunneling on the CBS-QB3 minimum energy profile predicts a unimolecular rate coefficient of 0.009 s^{-1} at 303 K, and 0.006 s^{-1} at 298K.

Table S6: barrier height (kcal/mol) for the 1,5-H-shift in 1-OH-2-OO-methacrolein.

Level of theory	Barrier height
B3LYP/6-31+G(d,p)	17.67
CBS-QB3	21.28
CBS-Q // QCISD/6-311G(d,p)	20.59
CBS-APNO	20.03

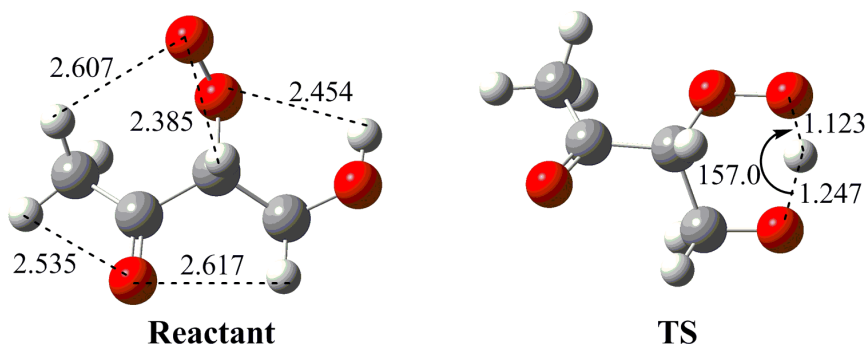
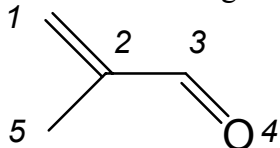


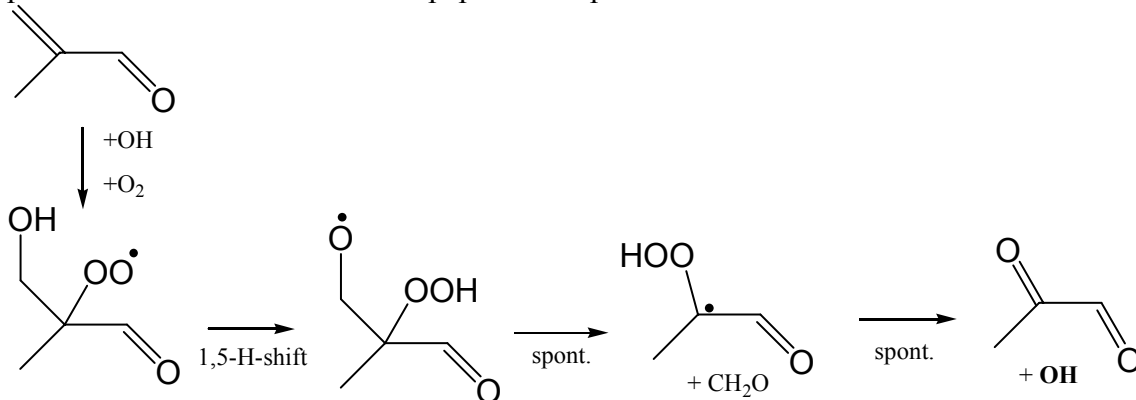
Figure S13: QCISD/6-311G(d,p) optimized geometries of the lowest-lying stationary points for the 1,5-H-shift in 4-OH-3-OO-MVK

Secondary chemistry: methacrolein

Labeling of methacrolein atoms is done here analogous to isoprene in the main paper:



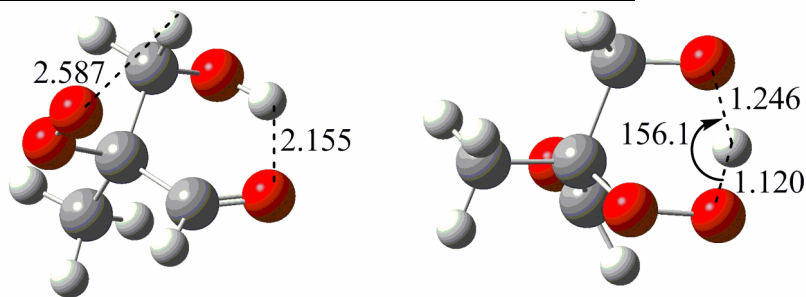
The OH-initiated oxidation of methacrolein might regenerate OH by an analogous process as described in the main paper for isoprene:



The barrier height for the H-shift is predicted at 19.7 kcal/mol. MC-TST calculations, incorporating WKB tunneling on the CBS-QB3 minimum energy profile predicts a unimolecular rate coefficient of 0.008 s^{-1} at 303 K, and 0.005 s^{-1} at 298K.

Table S7: barrier height (kcal/mol) for the 1,5-H-shift in 1-OH-2-OO-methacrolein.

Level of theory	Barrier height
B3LYP/6-31+G(d,p)	17.60
CBS-QB3	21.14
CBS-QB3 // QCISD/6-311G(d,p)	20.46
CBS-APNO	19.69



Reactant

TS

Figure S14: QCISD/6-311G(d,p) optimized geometries of the lowest-lying stationary points for the 1,5-H-shift in 1-OH-2-OO-methacrolein.